International Journal of Heat and Mass Transfer 52 (2009) 4317–4326

Contents lists available at ScienceDirect

International Journal of Heat and Mass Transfer

journal homepage: www.elsevier.com/locate/ijhmt

Multi-objective thermal design optimization and comparative analysis of electronics cooling technologies

Sidy Ndao, Yoav Peles, Michael K. Jensen *

Department of Mechanical, Aerospace, and Nuclear Engineering, Rensselaer Polytechnic Institute, Troy, NY 12180, USA

ARTICLE INFO

Article history:
Received 4 November 2008
Accepted 31 March 2009
Available online 20 May 2009

Keywords:
Micro-channel
Pin-fin
Offset strip fin
Jet impingement
Heat sink

ABSTRACT

A multi-objective thermal design optimization and comparative study of electronics cooling technologies is presented. The cooling technologies considered are: continuous parallel micro-channel heat sinks, in-line and staggered circular pin-fin heat sinks, offset strip fin heat sinks, and single and multiple submerged impinging jet(s). Using water and HFE-7000 as coolants, Matlab's multi-objective genetic algorithm functions were utilized to determine the optimal thermal design of each technology based on the total thermal resistance and pumping power consumption under constant pressure drop and heat source base area of 100 mm^2. Plots of the Pareto front indicate a trade-off between the total thermal resistance and pumping power consumption. In general, the offset strip fin heat sink outperforms the other cooling technologies.

1. Introduction

With increasing power density of electronic chips and devices, interest in effective cooling technologies has been growing both in industry and academia. Today, most research efforts are focused on single phase and flow boiling heat transfer in enhanced compact heat sink geometries such as micro-channels, micro pin fins, and impinging jets. Each of these technologies has its advantages and disadvantages [1], and the challenge is to find their optimal performance for a given electronics cooling application. As has been shown (e.g., [2–4]), given certain constraints, micro-channels, pin fins, and jet impingement cooling technologies have optimum design configurations whereby the total thermal resistance and power consumption are minimized. However, analytical comparison of these technologies against each other has not been performed.

1.1. Micro-channels

Since the pioneering work of Tuckerman and Pease [5] in 1981, many studies have been conducted on micro-channel heat sinks as summarized by Phillips [6] and, more recently, by Morini [7]. A number of studies have investigated the thermal design optimization of micro-channel heat sinks to determine the geometric dimensions that give optimum performance. Early analytical studies [8,9] showed the effect of the number of channels and fin thickness to channel width ratio on the thermal resistance. However, these studies were based on the classical analytical fin method, which may inaccurately predict the results for channel height to channel width ratio greater than 8 [10]. As an alternative to the classical analytical fin method, Kim and Hyun [11] proposed a porous media model based on an averaging method in which the heat sink was treated as a fluid-saturated porous medium. The results obtained from this model agreed with their numerical model [10]. Recently Kim and Kim [2] have proposed a closed-form total thermal resistance correlation for the thermal design optimization of micro-channels. Beside analytical models, several numerical methods have been used to study the thermal performance of micro-channels heat sinks [12–15].

1.2. Circular pin-fin and offset strip fin heat sinks

The literature on heat transfer and flow around circular pin-fins and offset strip fins is extensive as a result of more than 50 years of numerical and experimental investigations. Interested readers are referred to the work of Zukauskas [16,17], Kays and London [18], Manglik and Bergles [19], and Metzger et al. [20]. More recent studies on the thermal fluid characteristics of circular pin-fins and offset strip fins can be found in the works of Dong et al. [21], Won et al. [22], and Kosar et al. [23].

A number of studies have investigated the thermal design optimization of circular pin fins and offset strip fin heat sinks. Bejan and Morgan [24] reported the optimal geometry for an array of circular pin-fin and staggered offset strip fin heat sinks based on thermal resistance minimization. Based on their Darcy-flow porous medium, they concluded that the minimum thermal resistance of offset strip fin arrays is approximately half of the minimum ther-

* Corresponding author. Tel.: +1 518 276 2843; fax: +1 518 276 6025.
E-mail address: JenseM@rpi.edu (M.K. Jensen).

0017-9310/$ - see front matter © 2009 Elsevier Ltd. All rights reserved.
doi:10.1016/j.ijheatmasstransfer.2009.03.069

Nomenclature

a	offset strip fin length (m)
A	area (m^2)
A_b	total base area, heat source base area (m^2)
A_h	heat transfer area (m^2)
b	offset strip fin thickness (m)
$c_{p,f}$	specific heat (J/kg K)
d	diameter (m)
D_e	effective heat source diameter $\equiv (4A_b/\pi)^{1/2}$(m)
D_h	hydraulic diameter (m)
E	equality and inequality constraints
f	friction factor
G	volumetric flow rate (m^3/s)
h	average heat transfer coefficient (W/m^2 K)
H	fin height, distance between jet orifice plate and impingement surface (m)
j	Colburn j factor
k	thermal conductivity (W/m K)
k_e	total number of equality constraints
k_t	total number of equality and inequality constraints
K_c	coefficient of abrupt contraction
K_e	coefficient of abrupt expansion
L	length of heat sink in flow direction, length of heated area (m)
L_c	characteristic length (m)
L_{cj}	jet characteristic length $\equiv D_e/2$ (m)
l	jet orifice plate thickness (m)
m	exponent on θ in Nusselt number correlation
$\dot{m}$	mass flow rate (kg/s)
N	number of fins
n	exponent on φ in Nusselt number correlation
N_J	number of jet orifices
N_T	number of fins in lateral direction
N_L	number of fins in flow direction
Nu_d	Nusselt number based on diameter d
Nu_{D_h}	Nusselt number based on hydraulic diameter D_h
Nu_L	Nusselt number based on length L
P	power (W)
Pr	Prandtl number
$\dot{Q}$	heat input (W)
R	thermal resistance (K/W)
Re_d	Reynolds number based on diameter d
Re_{D_h}	Reynolds number based on hydraulic diameter D_h
Re_L	Reynolds number based on length L
S_j	jet-to-jet spacing (m)
S_T	circular pin fin lateral fin spacing (m)
S_L	circular pin fin streamwise fin spacing (m)
s	offset strip fin lateral fin spacing (m)
t	base thickness (m)
T	temperature (K)
U	velocity (m/s)
v_t	number of design variables
w_{ch}	micro-channel width (m)
w_w	micro-channel fin thickness (m)
W	width of heat sink (m)

Greek symbols

α	fin height to fin characteristic length L_c ratio
β	lateral fin spacing to fin characteristic length L_c ratio
δ	jet orifice plate thickness to jet diameter ratio $\equiv l/d_j$
Δp	pressure drop (Pa)
ε	porosity $\equiv w_{ch}/(w_{ch} + w_w)$
η_f	fin efficiency
η_o	overall heat sink efficiency
γ_{sf}	offset strip fin width to fin length ratio $\equiv b/a$
λ_{cp}	streamwise pitch $\equiv S_L/d_{cp}$
μ	viscosity (kg/m s)
φ	distance between orifice plate and impingement surface to jet diameter ratio
ρ	density (kg/m^3)
σ	unit frontal-area ratio
θ	jet-to-jet spacing to jet diameter ratio $\equiv S_j/d_j$

Subscripts

bulk	bulk
ch	channel
cond	conductive
conv	convective
cp	circular pin-fin
f	fluid
fin	fin
i	inlet
j	jet
k	equality and inequality constraints index
max	maximum
s	solid
sf	offset strip fin
tot	total
v	bounded constraints index

mal resistance of heat sinks with continuous fins. Other studies [3,19,25–27] have also shown that design variables such as fin dimensions, and longitudinal and transversal pitches have significant effects on the thermal performance.

1.3. Single and multiple submerged jet impingement

Jet impingement heat transfer has been studied extensively in the literature due to its high heat transfer coefficients at the stagnation zone, low pressure drops, and the elimination of interface thermal resistance between the chip and the cooling system [28]. Recently, several studies have focused on single and multiple microjet impingement heat transfer for electronics cooling applications [1]. However, only a few studies have been conducted to study their thermal design optimization. Jet-to-jet spacing to jet diameter ratio, and jet height to jet diameter ratios were both found to have significant effects on the thermal hydraulic performance of impinging jet(s) [29–31].

1.4. Comparison of cooling technologies

Despite the attention on the study of individual cooling technologies, less emphasis has been applied to comparing them and determining their suitability for a particular cooling application. This deficiency can be attributed to the challenging task of practically comparing different technologies, each with complex interactive relationships among their respective design variables. Nevertheless, a few researchers have attempted to compare these technologies [4,32–35]. These studies, however, either compared only the pin-fin cross-sections or were based on limited experimental data. The numerical comparisons are often simplified (e.g., 2-D domain) and, therefore, did not take into account fin height. Most of the existing comparative studies were also carried out using parametric or single objective optimization comparisons. As this present work will show, single objective optimization (e.g., thermal resistance or pumping power) may not necessarily yield optimum performance.

The multi-objective thermal design optimization and comparative analysis of electronics cooling technologies undertaken in the present work is effectuated in two steps: (1) each cooling system is optimized separately by simultaneous minimization of the total thermal resistance and the pumping power consumption under imposed constraints; and (2) based on their optimum design, the cooling systems are then compared.

2. Optimization technique and thermal design models

2.1. Optimization metrics and design variables

Fig. 1 shows the different cooling technologies considered in the present study along with their respective design variables. The cooling systems consist of micro-channel, in-line and staggered circular pin-fin, offset strip fin heat sinks, single and multiple impinging jet(s). Two metrics, namely the total thermal resistance and power consumption, are simultaneously optimized under constant pressure drop for each of the separate cooling technologies. The total thermal resistance is defined as:

$$R_{tot} = R_{cond} + R_{conv} + R_{bulk} = \frac{T_{s,\max} - T_{f,i}}{\dot{Q}} \tag{1}$$

$$R_{cond} = \frac{t}{k_s A_b}, \quad R_{conv} = \frac{1}{\eta_o h A_h}, \quad R_{bulk} = \frac{1}{\rho_f c_{p,f} G} \tag{2}$$

The power consumption is evaluated simply as:

$$P = G \cdot \Delta p \tag{3}$$

The total thermal resistance models and design variables used in the present study are presented in Table 1.

2.2. Heat transfer and friction factor models

The heat transfer and friction factor models along with their experimental or analytical conditions used in the present study are summarized in Table 2. These models have been selected after a rigorous review of the existing relevant analytical and experimental correlations in the literature. Each of these models has been validated by their respective authors and were chosen based on each individual correlation's generality (e.g., parameter space range), ability to predict the optimization results more accurately, and convenience (e.g., coolant). Heat transfer models are presented in terms of the Nusselt number, *Nu*, and Colburn factor, *j*, whereas the pressure drop for micro-channel and offset strip fin heat sinks [18] is defined as:

$$\Delta p = \frac{\rho_f U^2}{2}\left[(K_c + 1 - \sigma^2) + f\left(\frac{4L}{D_h}\right) - (1 - \sigma^2 - K_e)\right] \tag{4}$$

For circular pin-fin heat sinks [37], the expression is:

$$\Delta p = \frac{\rho_f U^2}{2}\left[(K_c + 1 - \sigma^2) + fN_{L_{cp}} - (1 - \sigma^2 - K_e)\right] \tag{5}$$

and for single and multiple jet impingement cooling [38], the expression is:

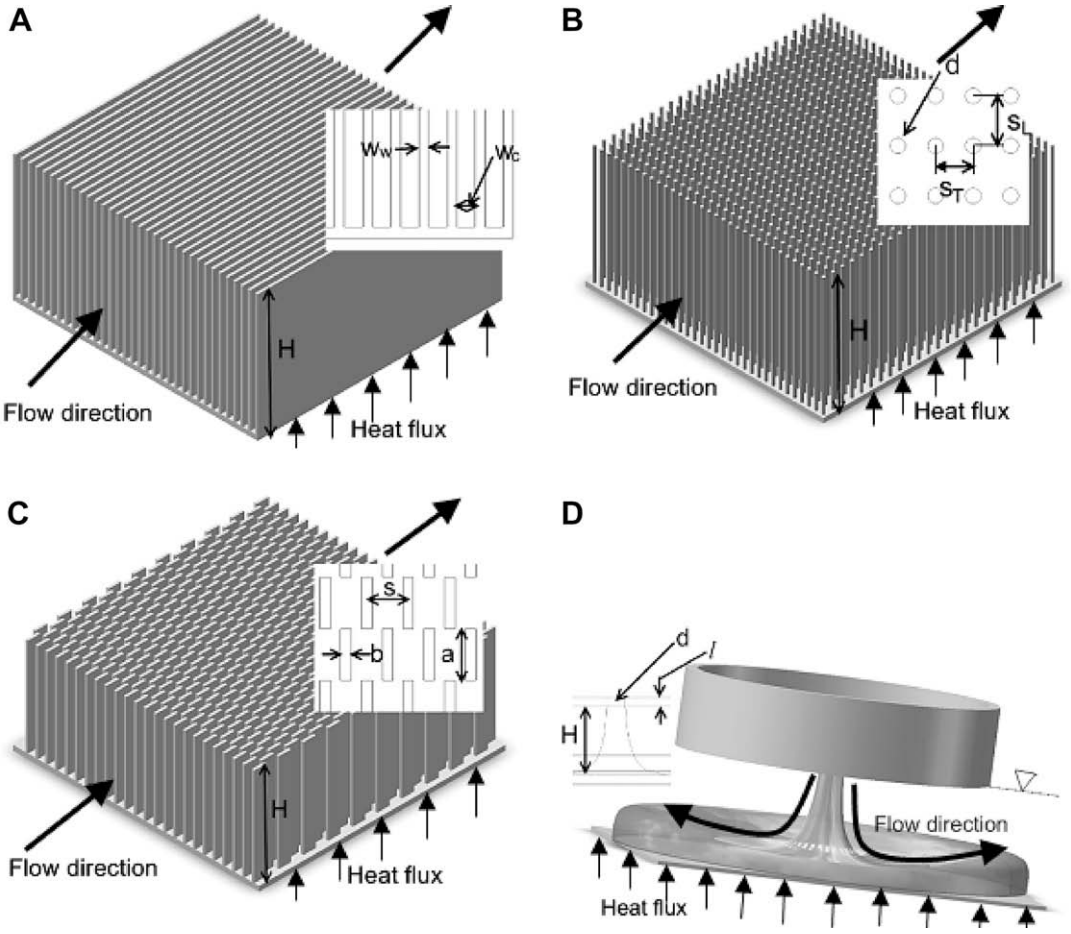

Fig. 1. (A) Schematic model of micro-channel heat sink. (B) Schematic model of circular pin-fin heat sink. (C) Schematic model of offset strip fin heat sink. (D) Schematic model of jet impingement cooling.

Table 1
Total thermal resistance models and design variables used in the present study.

	Design variables	Total thermal resistance
Micro-channel heat sink [2]	$\alpha_{ch}, \beta_{ch}, w_{ch}$	$R_{tot} = \frac{1}{3}\frac{(1+\beta_{ch})\alpha_{ch}w_{ch}}{k_s\beta_{ch}LW} + \frac{17}{140}\frac{w_{ch}(1+\beta_{ch})}{k_f\alpha_{ch}LW} + \frac{\sqrt{12\mu_f w_{ch}(1+\beta_{ch})L}}{\rho_f c_{p,f}\sqrt{w_{ch}^4\alpha_{ch}WP}} + \frac{t}{k_s}\frac{1}{LW}$
Circular pin-fin heat sink (current work)	$\alpha_{cp}, \beta_{cp}, \lambda_{cp}, d_{cp}$	$R_{tot} = \frac{\left(\frac{1}{Nu_{d_{cp}}k_f}\frac{1}{\pi\eta_f}\frac{\beta_{cp}\lambda_{cp}d_{cp}}{\alpha_{cp}}\frac{1}{LW}\right)\cdot\left(\frac{1}{Nu_L k_f}\frac{L}{1-[\pi/(4\beta_{cp}\lambda_{cp})]}\frac{1}{LW}\right)}{\left(\frac{1}{Nu_{d_{cp}}k_f}\frac{1}{\pi\eta_f}\frac{\beta_{cp}\lambda_{cp}d_{cp}}{\alpha_{cp}}\frac{1}{LW}\right)+\left(\frac{1}{Nu_L k_f}\frac{L}{1-[\pi/(4\beta_{cp}\lambda_{cp})]}\frac{1}{LW}\right)} + \frac{L}{c_{p,f}\mu_f}\frac{4}{\mathrm{Re}_{Dh_{cp}}}\frac{(\beta_{cp}-1)\lambda_{cp}}{\pi\alpha_{cp}}\frac{1}{LW} + \frac{t}{k_s}\frac{1}{LW}$
Offset strip fin heat sink (current work)	$\alpha_{sf}, \beta_{sf}, \gamma_{sf}, a$	$R_{tot} = \frac{D_{h_{sf}}}{\eta_o Nu_{Dh_{sf}}k_f\{LW+\{a^2N_{sf}[(2\alpha_{sf}(1+\gamma_{sf}))-\gamma_{sf}]\}\}} + \frac{WL^2}{a^2c_{p,f}\mu_f}\frac{1}{\mathrm{Re}_L}\frac{1}{N_{sf}\alpha_{sf}(\beta_{sf}-\gamma_{sf})}\frac{1}{LW} + \frac{t}{k_s}\frac{1}{LW}$
Jet impingement cooling (current work)	$\delta, \theta, \varphi, d_j$	$R_{tot,single} = \frac{d_j}{Nu_j k_f LW} + \frac{4}{c_{p,f}\mathrm{Re}_{d_j}\mu_f\pi d_j} + \frac{t}{k_s}\frac{1}{LW}$ $R_{tot,multiple} = \frac{L_{cj}}{Nu_{L_{cj}}k_f LW} + \frac{4}{c_{p,f}\mathrm{Re}_{d_j}\mu_f\pi N_j d_j} + \frac{t}{k_s}\frac{1}{LW}$

Table 2
Heat transfer and friction factor models used in the present study.

	Nussult Number correlations	Friction factor correlations	Geometric and operating conditions
Micro-channel heat sink [2]	$Nu_{ch} = \frac{1}{3(1-\varepsilon)}\left(\frac{k_f}{k_s}\right) + \frac{17}{140\varepsilon x_{ch}^2}$	$f\mathrm{Re}_{D_{h_{ch}}} = 24\left(\frac{\alpha_{ch}}{\alpha_{ch}+1}\right)^2$	$\alpha_{ch} > 4, k_s/k_f > 20$ $L/D_{h_{ch}} > 0.05\mathrm{Re}_{D_{h_{ch}}}$ $L/D_{h_{ch}} > 0.05\mathrm{PrRe}_{D_{h_{ch}}}$
Circular pin-fin heat sink [3]	$Nu_{d_{cp}} = C_1\mathrm{Re}_{d_{cp}}^{1/2}\mathrm{Pr}^{1/3}$ $C_{1,in-line} = \frac{[0.2+\exp(-0.55\beta_{cp})]\beta_{cp}^{0.785}\lambda_{cp}^{0.212}}{(\beta_{cp}-1)^{0.5}}$ $C_{1,staggered} = \frac{0.61\beta_{cp}^{0.591}\lambda_{cp}^{0.053}}{(\beta_{cp}-1)^{0.5}[1-2\exp(-1.09\beta_{cp})]}$	$f = K_{inline}[0.233 + 45.78/(\beta_{cp}-1)^{1.1}\mathrm{Re}_{d_{pc}}]$ $K_{inline} = 1.009[(\beta_{cp}-1)/(\lambda_{cp}-1)]^{1.09/\mathrm{Re}_{d_{cp}}^{0.0553}}$ $f = K_{staggered}(378.6/\beta_{cp}^{13.1/\beta_{cp}})/\mathrm{Re}_{d_{cp}}^{0.68/\beta_{cp}^{1.29}}$ $K_{staggered} = 1.175[\lambda_{CP}/(\beta_{cp}\mathrm{Re}_{d_{cp}}^{0.3124})] + 0.5\mathrm{Re}_{d_{cp}}^{0.0807}$	$\mathrm{Pr} \geq 0.71$ $40 \leq \mathrm{Re}_{d_{cp}} \leq 1000$ $1 \leqslant U(m/s) \leqslant 6$ $1 \leq d(mm) \leq 3$ $1.25 \leq \lambda_{cp} \leq 3$ $1.25 \leq \beta_{cp} \leq 3$ All gases and most liquid with moderate Pr
Offset strip fin heat sink [19]	$Nu_{Dh_{sf}} = j\mathrm{Re}_{D_{h_{sf}}}\mathrm{Pr}^{1/3}$ $j = 0.6522\mathrm{Re}_{D_{h_{sf}}}^{-0.5403}\left(\frac{\beta_{sf}-\gamma_{sf}}{\alpha_{sf}}\right)^{-0.1541}\gamma_{sf}^{0.1499}\left(\frac{\gamma_{sf}}{\beta_{sf}-\gamma_{sf}}\right)^{-0.0678}$ $\times\left[1+5.269\cdot10^{-5}\mathrm{Re}_{D_{h_{sf}}}^{1.340}\left(\frac{\beta_{sf}-\gamma_{sf}}{\alpha_{sf}}\right)^{0.504}\lambda_{sf}^{0.456}\left(\frac{\gamma_{sf}}{\beta_{sf}-\gamma_{sf}}\right)^{-1.055}\right]^{0.1}$	$f = 9.6243\mathrm{Re}_{D_{h_{sf}}}^{-0.7422}\left(\frac{\beta_{sf}-\gamma_{sf}}{\alpha_{sf}}\right)^{-0.1856}\gamma_{sf}^{0.3053}\left(\frac{\gamma_{sf}}{\beta_{sf}-\gamma_{sf}}\right)^{-0.2659}$ $\times[1+7.669\cdot10^{-8}\mathrm{Re}_{D_{h_{sf}}}^{4.429}\left(\frac{\beta_{sf}-\gamma_{sf}}{\alpha_{sf}}\right)^{0.920}\lambda_{sf}^{3.767}\left(\frac{\gamma_{sf}}{\beta_{sf}-\gamma_{sf}}\right)^{0.236}]^{0.1}$	
Jet impingement cooling [31,36]	$Nu_{d_j,\mathrm{single}} = 0.926\mathrm{Re}_{d_j}^{0.535}\mathrm{Pr}^{0.452}\delta^{-0.07}\left(\frac{D_e}{d_j}\right)^{-0.385}$ $Nu_{L_{cj},multiple} = 23.39\mathrm{Re}_{d_j}^{0.46}\mathrm{Pr}^{0.4}\theta^m\phi^n$ $\left.\begin{matrix}m=-0.442\\n=-0.00716\end{matrix}\right\}2\leq\phi\leq3,\ \left.\begin{matrix}m=-0.121\\n=-0.427\end{matrix}\right\}5\leq\phi\leq20$	$f(\mathrm{Re}_{d_j} > 2300) = \frac{0.079}{\mathrm{Re}_{d_j}^{1/4}}$ $f(\mathrm{Re}_{d_j} \leq 2300) = \frac{16}{\mathrm{Re}_{d_j}}$	Single : $1.59 \leq d_j \leq 6.35mm$ $7.1 \leq \mathrm{Pr} \leq 25.2$ $4000 \leq \mathrm{Re}_{d_j} \leq 23000$ $D_e = 11.28mm$

$$\Delta p = \frac{\rho_f U^2}{2}\left[(K_c + 1 - \sigma^2) + f\left(\frac{4l}{d_j}\right) + 1\right] \tag{6}$$

The definitions of α, β, σ, D_h, and G for each of the cooling technologies are tabulated in Table 3. The coefficients of abrupt contraction and expansion, K_c and K_e, correlated from the graphs in [18] for micro-channels, offset strip fins, and jet impingement configurations are given by:

$$\begin{aligned} K_c &= -0.4446\sigma^2 + 0.0487\sigma + 0.7967 \\ K_e &= 0.9732\sigma^2 - 2.3668\sigma + 0.9973 \end{aligned} \tag{7}$$

while for circular pin fins [37], the following expressions are used:

$$\begin{aligned} K_c &= -0.03116\sigma^2 - 0.3722\sigma + 1.0676 \\ K_e &= 0.9301\sigma^2 - 2.5746\sigma + 0.973 \end{aligned} \tag{8}$$

2.3. Optimization procedures

Each system is optimized separately through a multi-objective optimization of the total thermal resistance and pumping power

Table 3
Definition of some common terms used in the present study.

	α	β	σ	$D_h(m)$	$G(m^3/s)$
Micro-channel heat sink	$\frac{H_{ch}}{w_{ch}}$	$\frac{w_w}{w_{ch}}$	$\frac{1}{\beta_{ch}+1}$	$\frac{2\alpha_{ch}w_{ch}}{\alpha_{ch}+1}$	$N_{ch}\alpha_{ch}w_{ch}^2U$
Circular pin-fin heat sink	$\frac{H_{cp}}{d_{cp}}$	$\frac{S_T}{d_{cp}}$	$\frac{\beta_{cp}-1}{\beta_{cp}}$	$\frac{4d_{cp}(\beta_{cp}-1)\lambda_{cp}}{\pi}$	$N_{T_{cp}}\beta_{cp}\alpha_{cp}d_d^2U$
Offset strip fin heat sink	$\frac{H_{sf}}{a}$	$\frac{s}{a}$	$\frac{\beta_{sf}-\gamma_{sf}}{\beta_{sf}}$	$\frac{2(\beta_{sf}-\gamma_{sf})\alpha_{sf}a}{(\beta_{sf}-\gamma_{sf})+\alpha_{sf}+\alpha_{sf}\gamma_{sf}}$	$N_{T_{sf}}\alpha_{sf}(\beta_{sf}-\gamma_{sf})a^2U$
Jet impingement cooling			$\frac{\pi d_j^2}{4LW}N_J$		$\frac{\pi d_j^2}{4}UN_J$

Table 4
Heat sink and coolant properties.

Heat sink/Solid	L	10 mm	
	W	10 mm	
	t	0.1 mm	
	k_s	148 W/m K	
	ρ_s	2.33×10^3 kg/m^3	
		Water	HFE-7000
Coolants	k_f	0.60 W/m K	0.074 W/m K
	$c_{p,f}$	4179 J/kg K	1062 J/kg K
	ρ_f	997.1 kg/m^3	1414 kg/m^3
	μ_f	8.91×10^{-4} kg/m s	4.25×10^{-4} kg/m s
	Pr	6.21	6.07

under constant pressure drop and a fixed heat source base area of 100 mm^2. The heat sinks are made from silicon because of its high thermal conductivity and also because it is the most commonly used semiconductor in microelectronics. Water and HFE-7000, with constant properties assumption, are chosen as the coolants. The thickness of the heated areas is kept fixed while the cooling systems' respective design variables are allowed to vary within imposed bounds.

For a given pressure drop, Δp, the velocity, U, is iteratively solved from the pressure drop and friction factor equations. Once the velocity is known, the total thermal resistance and pumping power are easily computed.

Using Matlab's multi-objective genetic algorithm [39], both the total thermal resistance and pumping power consumption are simultaneously minimized. Consider the vector:

$$\vec{F}(\vec{X}) = [F_1(\vec{X}), F_2(\vec{X})] \tag{9}$$

where the competing objective functions $F_1(\vec{X})$ and $F_2(\vec{X})$ represent the total thermal resistance and pumping power, respectively, and the vector $\vec{X}$ denotes the design variables. The goal of the multi-objective optimization is to minimize the objective vector $\vec{F}(\vec{X})$ under a number of constraints and bounds. The mathematical representation of the problem may then be written as:

$$\begin{aligned} &\min_{\vec{X}} \vec{F}(\vec{X}) \\ &\text{subjected to} \\ &E_k(\vec{X}) \le 0 \quad k = 1, \cdots, k_e \\ &E_k(\vec{X}) = 0 \quad k = k_e, \cdots, k_t \\ &lb_v \le X_v \le ub_v \quad v = 1, \cdots, v_t \end{aligned} \tag{10}$$

Matlab's multi-objective function, *gamultiobj*, was called to solve the above problem. The function's arguments consist of the objective functions and the parameter space along with some genetic algorithm options such as population size, Pareto fraction, and plot function. The computed results consist of sets of non-inferior solutions. Non-inferior solutions are sets of optimal solutions in which an improvement in one objective requires a degradation of another.

Tables 4 and 5 show the properties of the coolants, heat sink materials, and the values of the imposed optimization constraints used in the present study. In defining the parameter space, care was taken not to over-extrapolate the heat transfer and friction factor models.

Table 5
Optimization constraints used in the present study.

	Design variables constraints	Pressure drop
Micro-channel heat sink	$50{\cdot}10^{-6} \le w_{ch} \le 600{\cdot}10^{-6}$ m $4 \le \alpha_{ch} \le 50$ $0.1 \le \beta_{ch} \le 1.0$	30 kPa–90 kPa
Circular pin-fin heat sink	$100 \times 10^{-6} \le d_{cp} \le 2 \times 10^{-3}$ m $4 \le \alpha_{cp} \le 20$ $1.25 \le \beta_{cp} \le 3$ $1.25 \le \lambda_{cp} \le 3$	30 kPa–90 kPa
Offset strip fin heat sink	$100 \times 10^{-6} \le a \le 2 \times 10^{-3}$ m $2 \le \alpha_{sf} \le 5$ $0.2 \le \beta_{sf} \le 0.8$ $0.03 \le \gamma_{sf} \le 0.08$	30 kPa–90 kPa
Jet impingement cooling	$0.8 \le d_j \le 3.0$ mm $0.25 \le \delta \le 12$ $3 \le \theta \le 7$ $2 \le \varphi \le 3$	30 kPa–90 kPa

3. Results and discussion

3.1. Validation of models

As mentioned earlier, the heat transfer and friction factor models used in the present study have been developed and validated by their respective authors. However, to validate the calculation approach used in the present work, calculated thermal resistances are compared against experimental results. As shown in Table 6, the calculated results agree with the experimental values.

3.2. Multi-objective optimization and Pareto optimal solutions

The multi-objective solution yields a set of optimal solutions in which an improvement in one objective requires a degradation of another. The plots of these optimal solutions with water are shown in Figs. 2A, 3A, 4A, 5A, 6A, and 7A. These curves are known as the Pareto front and show a clear trade-off between the total thermal resistance and power consumption; an improvement (a decrease) in the total thermal resistance results in an increase in the power consumption. The Pareto front also indicates that the nature of this trade-off is not uniform. As illustrated in Fig. 2A, for total thermal resistances less than 0.25 K/W, increasing the total thermal resistance gradually decreases the pumping power. However, at total thermal resistance values larger than 0.25 K/W, further increasing the total thermal resistance does not produce any significant improvement to the power consumption. Similarly, at relatively small pumping powers, and depending on the pressure drop, increasing the pumping power will decrease the total thermal resistance until it reaches a condition where any further increase of the pumping power will not have any significant effect on the total thermal resistance. It is evident from the above discussion that for a given pressure drop, the design variables corresponding

Table 6
Comparison of thermal resistances.

	Parameters used in calculations	R(K/W)	
		Experimental	Calculated
Micro-channel heat sink [40] (Table 2)	Water, $L = W = 10$ mm, $w_{ch} = 56$ μm, $\alpha_{ch} = 5.7$, $\beta_{ch} = 0.78$, $t = 213$ μm, $G = 4.7$ cm^3/s	0.11	0.10
Circular pin-fin heat sink [41]	Water, $L = 10$ mm, $W = 1.8$ mm, $d_{cp} = 100$ μm, $\alpha_{cp} = 2.43$, $\beta_{cp} = \lambda_{cp} = 1.5$, $\Delta p = 14.7$ kPa	~5.8	5.7
Offset strip fin heat sink [42]	Air, $L = 100$ mm, $W = 50$ mm $a = 3.24$ mm, $\alpha_{sf} = 3.08$, $\beta_{sf} = 1.179$, $\gamma_{sf} = 0.268$, $\dot{m} = 4x10^{-3}$ kg/s	~0.17	0.18
Jet impingement cooling [31]	Water, $d_j = 1.0$ mm, $\theta = 7$, $\phi = 2$, $\mathrm{Re}_{d_j} = 3000$, $A_h = 780$ mm^2	~0.044	0.041

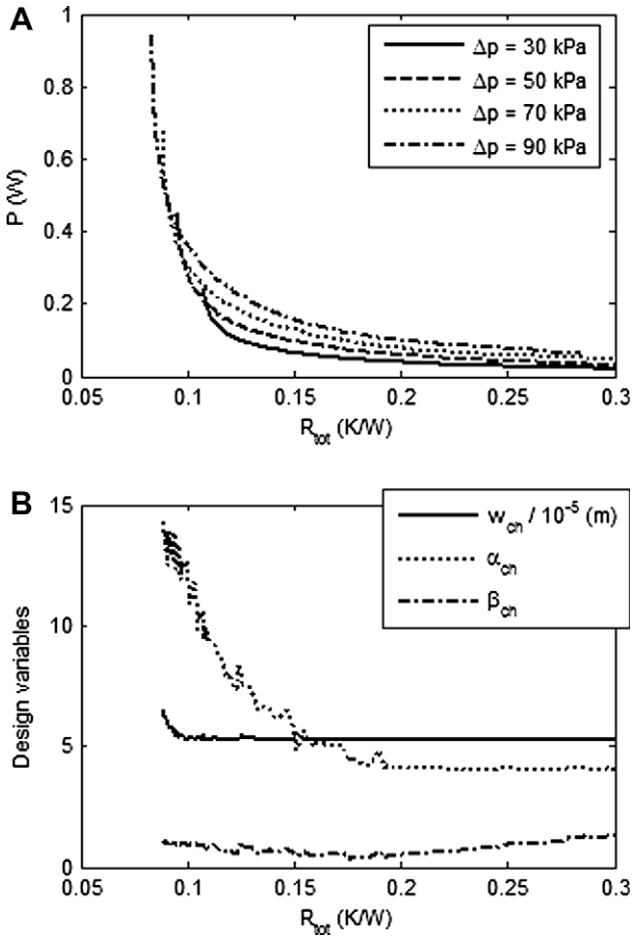

Fig. 2. (A) Micro-channel heat sink Pareto optimal solutions for water. (B) Distribution of the micro-channel heat sink design variables along its Pareto front for water at Δp = 70 kPa.

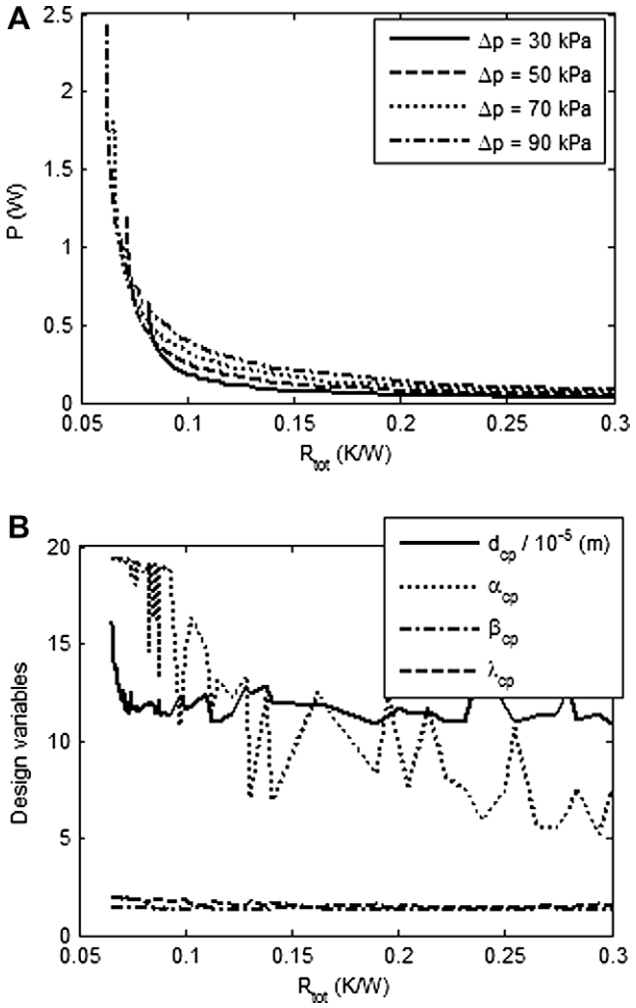

Fig. 3. (A) In-line circular pin-fin heat sink Pareto optimal solutions for water. (B) Distribution of in-line circular pin-fin heat sink design variables along its Pareto front for water at Δp = 70 kPa.

to the lowest thermal resistance do not necessarily correspond to those of the lowest power consumption and vice versa.

A deeper insight into this trade-off can be gained by studying the effects of individual design variables on the total thermal resistance and power consumption. Taking the offset strip fin heat sink as an example, the total thermal resistance decreases with increasing aspect ratio, α_{sf}. This happens because as α_{sf} increases, the total heat transfer area increases. Conversely, the power consumption will increase with increasing α_{sf} and fin length. This is because for a constant pressure drop, increasing α_{sf} would increase the volumetric flow rate and consequently increase the power consumption.

The role of pressure drop on the optimal heat sink design for a particular electronics cooling application can be also observed from these figures. As illustrated in Fig. 3A, at relatively low pumping powers, below 0.3 W, the lowest thermal resistance is achieved with the lower pressure drop of 30 kPa. However, at higher pumping power values, the lowest thermal resistance is achieved at higher pressure drops. In offset strip fins (Fig. 5A), the effect of pressure drop is somewhat limited to relatively large values of the optimal thermal resistance. For total thermal resistances less than 0.05 K/W, increasing the pressure drop will not significantly improve the thermal resistances for a given power consumption. As for impinging jet(s) (Figs. 6A and 7A), an increase in the pressure drop considerably reduces the total thermal resistance. This is due to the relatively low friction factor associated with jet impingement, which allows for a high Reynolds number, and thus enhancement of the heat transfer coefficients. For a given flow velocity, impinging jet(s) have smaller pressure drops compared to parallel flow heat sink configurations. This, thereby, explains why the effect of pressure drop on impinging jet(s) is more significant.

Figs. 2B, 3B, 4B, 5B, 6B, and 7B show the distribution of the cooling systems' design variables along their respective Pareto optimal fronts for water at Δp = 70 kPa. Note that dimensions have been divided by a constant so that all design variables could easily be seen on a simple plot. As shown in these figures, the distribution of the cooling system's respective design variables is complex. For the case of the micro-channel heat sink (Fig. 2B), it is observed that the optimal channel width does not vary significantly along the Pareto optimal front. This optimal channel width is calculated to be approximately on average 60 μm. On the other hand, the aspect ratio, α_{ch}, decreases continuously along the Pareto optimal front with increasing optimal thermal resistances, while β_{ch} shows both decreasing and increasing behaviors. More pronounced fluctuating characteristics of design variables along their respective Pareto optimal fronts can be seen in circular pin fins (Figs. 3B and 4B) and offset strip fins (Fig. 5B). In Fig. 7B, the jet diameter shows an almost non-varying characteristic. This behavior is a direct result of the imposed constraints on the jet diameter.

Plots of the distribution of the cooling systems' design variables along their respective Pareto optimal fronts for Δp = 30 kPa have shown similar trends, however with different magnitudes.

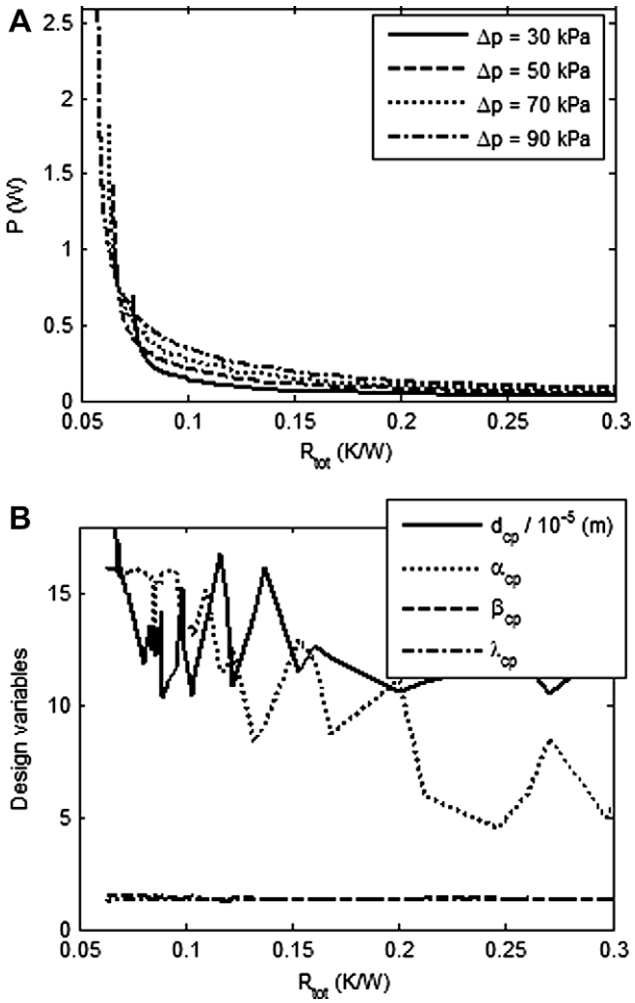

Fig. 4. (A) Staggered circular pin-fin heat sink Pareto optimal solutions for water. (B) Distribution of staggered circular pin-fin heat sink design variables along its Pareto front for water at Δp = 70 kPa.

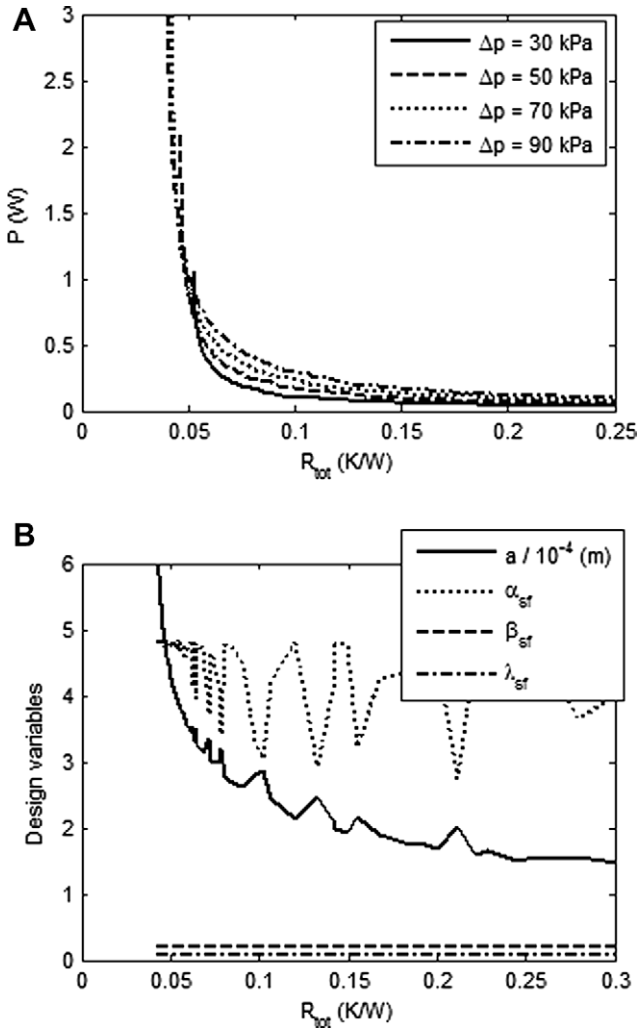

Fig. 5. (A) Offset strip fin heat sink Pareto optimal solutions for water. (B) Distribution of offset strip fin heat sink design variables along its Pareto front for water at Δp = 70 kPa.

It is important to note that points along a single Pareto front (e.g., fixed pressure drop) do not necessarily correspond to fixed design variables. Likewise, for a given total thermal resistance or pumping power, the design variables are not necessarily fixed from one pressure drop curve to another. Therefore, one cannot easily decouple the effects of the Reynolds number and the effects of the friction factors, which makes it very difficult to physically explain some of the trends discussed earlier.

In light of the above paragraph, the simplest scenario to analyze may be the case of the multiple impinging jets. As illustrated in Fig. 7A, at relatively low pumping powers, the lowest thermal resistance is achieved with the lower pressure drop. This may be because for a fixed relatively low pumping power, the flow rate is relatively higher for lower pressure drops. However, this is not the case for relatively higher pumping powers as the lower pressure drops cannot permit high flow rate as a result of the friction factors' effects, which slope decreases with increasing Reynolds number.

Also very interesting to note is that as a result of the pressure drop curves cross-overs, the lowest pumping power consumption does not necessarily occur at the lowest pressure drop for a given total thermal resistance value. This observation can be easily verified by drawing a vertical line around the proximity of a pressure drop curves cross-over (e.g., R_{tot} = 0.18 K/W in Fig. 6A). This will result to a pumping power curve in which the optimum pumping power (minimum pumping power) may not necessarily occur at the lowest pressure drop. These pressure drop curves cross-overs are not only specific to the current study but have been observed by previous researchers such as Bar-Cohen et al. [43].

Depending on the cooling needs, designers can rely on the combination of the abovementioned plots (Figs. 2–7) to determine the optimal design of a cooling system. Some of these optimum solutions are also tabulated in Table 7.

3.3. Comparison among the cooling technologies

Figs. 8 and 9 show comparisons of the cooling technologies considered in this study based on their respective Pareto optimal solutions at two different pressure drops with water. For a given pressure drop of 30 kPa and heat source base area of 100 mm^2 (Fig. 8), the offset strip fin heat sink offers the best thermal hydraulic performance. The relatively better performance of the offset strip fin heat sink can be attributed to its ability to enhance the heat transfer coefficients as well as to add surface area. In offset strip fins, the thermal boundary layers are stripped and reestablished; this causes the average heat transfer coefficients to be higher than those of continuous parallel plate fins. Besides interrupting the growth of the thermal boundary layers, offset strip fins may cause vortex shedding [44], which may increase the heat transfer coefficients [45]. However, this enhancement of the heat transfer

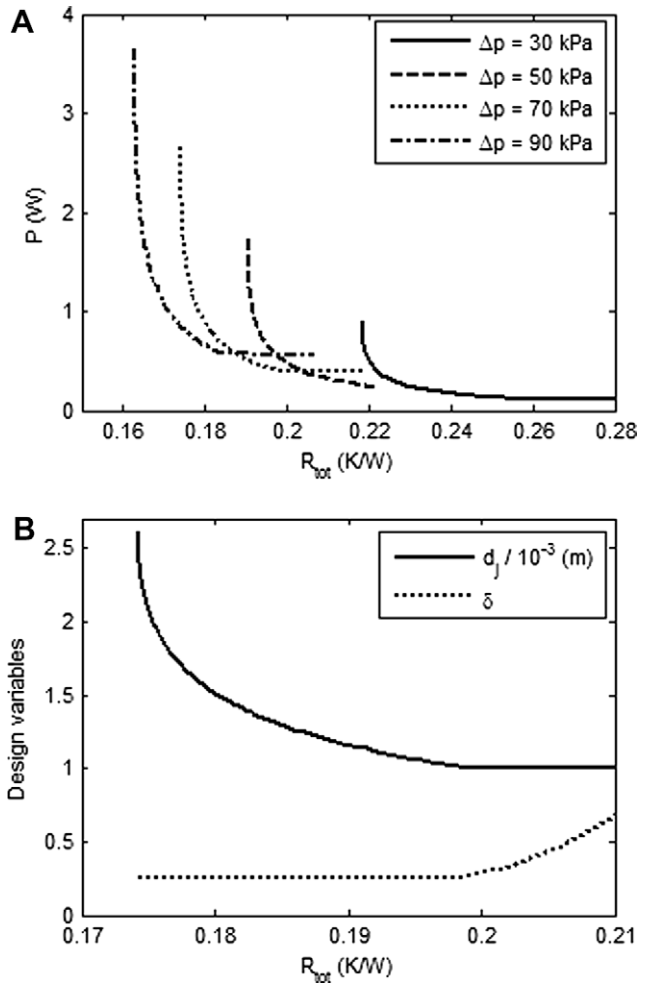

Fig. 6. (A) Single jet impingement Pareto optimal solutions for water. (B) Distribution of single jet impingement design variables along its Pareto front for water at Δp = 70 kPa.

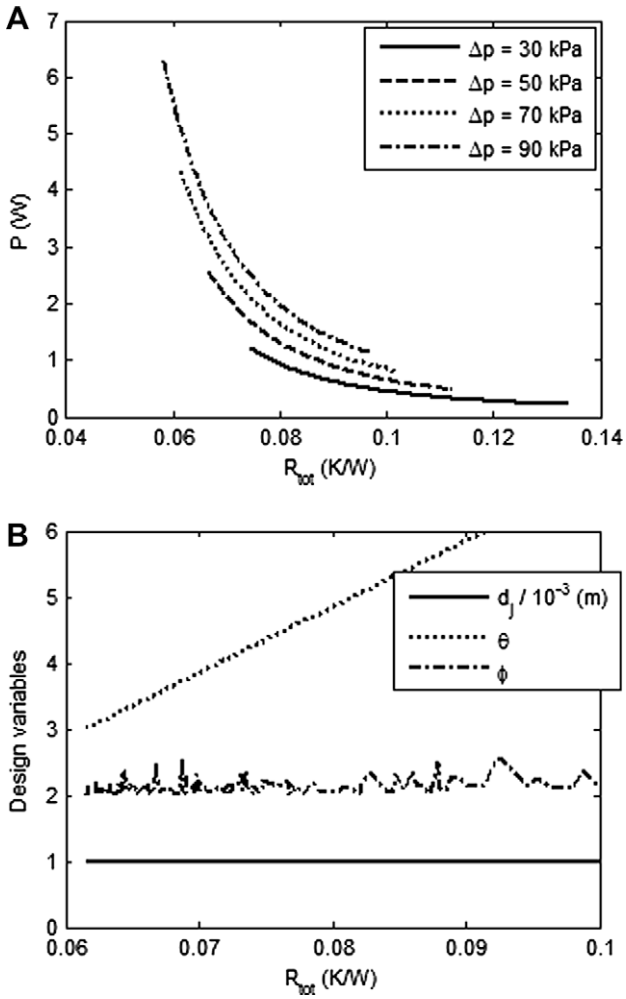

Fig. 7. (A) Multiple jet impingement Pareto optimal solutions for water. (B) Distribution of multiple jet impingement design variables along its Pareto front for water, Δp = 70 kPa.

coefficients is also associated with higher pressure drop and, consequently, higher pumping power consumption.

Next to the offset strip fin heat sink in performance are the staggered and in-line circular pin-fin heat sinks, with the staggered arrangement displaying slightly better performance than the in-line arrangement. The heat transfer coefficients of circular pin fins are higher than those of continuous parallel plate fins. This is due to the relatively small boundary layer thickness over the surface of the pin fins and the bulk mixing within the tube bundles. In comparison to the staggered pin-fin arrangement, the thermal performance of the in-line arrangement is slightly lower. Zukauskas and Ulinskas [17] came to a similar conclusion that in-line arrangements have lower heat transfer coefficients with, however, less hydraulic resistance as compared to staggered arrangements. For relatively very low pumping powers, below 0.05 W, micro-channel heat sinks offer the lowest thermal resistance.

The performance of multiple impinging jets is obviously better than that of a single impinging jet. The heat transfer coefficients in a single liquid impinging jet are very high at the stagnation zone; however, they decrease rapidly away from the stagnation point. To overcome this fall-off, multiple jets are used. In most of the cases studied, as shown in Fig. 8, the parallel flow heat sinks outperform jet impingement cooling. Even though jet impingement cooling yields very high heat transfer coefficients, its heat transfer area is much smaller compared to parallel flow heat sinks, and, therefore, the product hA_h is smaller. Lee and Vafai [4] have shown

Table 7
Multi-objective optimization results for Δp = 70 kPa (dimensions in μm).

	a	d	w_c	α	β	λ_{cp}	γ_{sf}	θ	φ	P (W)	R_{tot} (K/W)
Micro-channel heat sink			65	14.3	0.98					0.67	0.088
In-line circular pin-fin heat sink		162		19.4	1.42	1.93				1.81	0.065
Staggered circular pin-fin heat sink		196		16.1	1.56	1.25				1.82	0.063
Offset strip fin heat sink	729			4.82	0.20		0.079			4.14	0.042
Single jet impingement[a]		2614								2.66	0.174
Multiple jet impingements		997						3.0	2.0	6.28	0.058

[a] δ = 0.25.

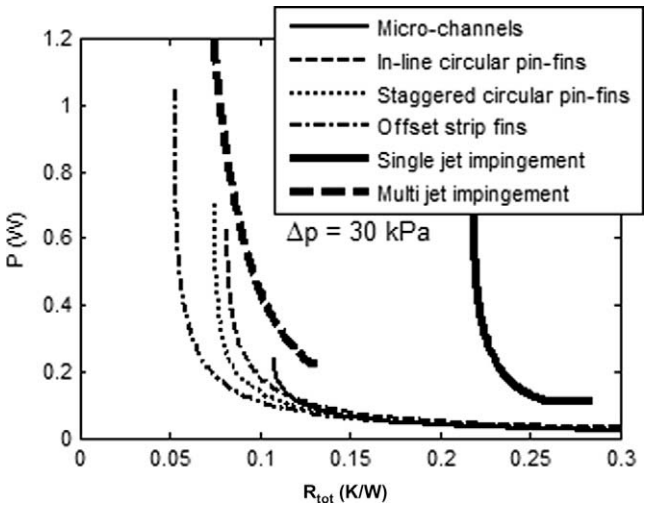

Fig. 8. Pareto optimal solutions at $\Delta p = 30$ kPa for water.

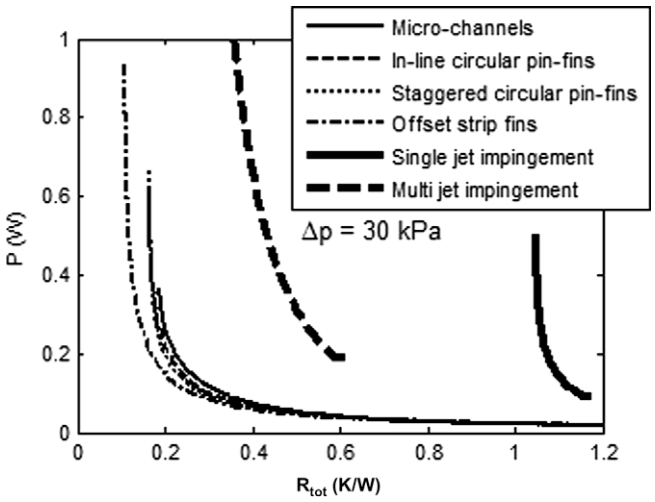

Fig. 10. Pareto optimal solutions at $\Delta p = 30$ kPa for HFE-7000.

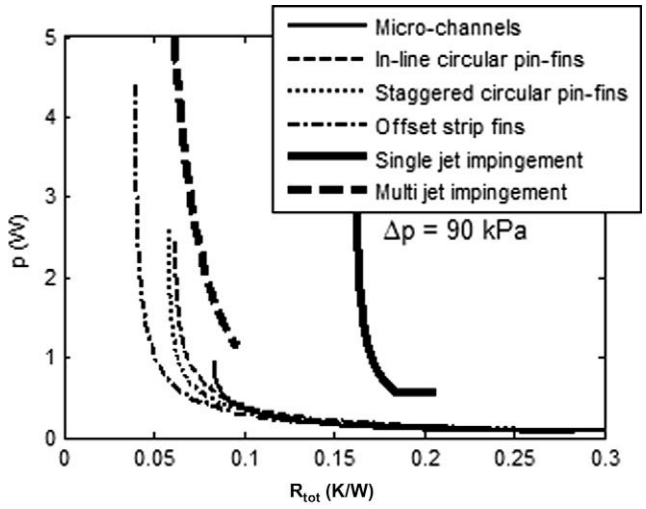

Fig. 9. Pareto optimal solutions at $\Delta p = 90$ kPa for water.

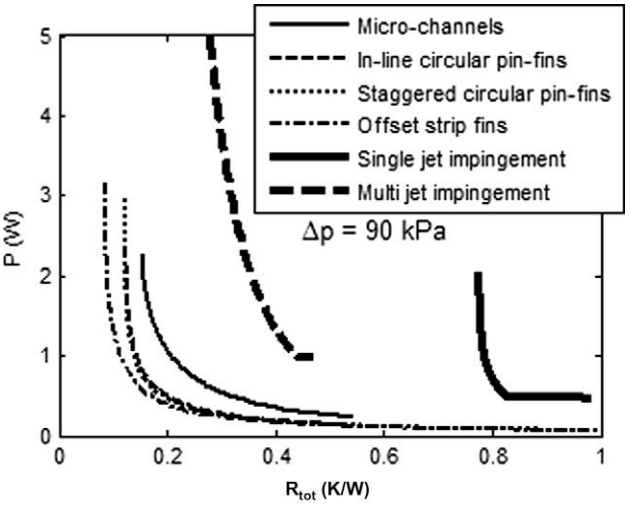

Fig. 11. Pareto optimal solutions at $\Delta p = 90$ kPa for HFE-7000.

that micro-channel heat sinks can perform better or worse than multiple jet impingement cooling depending on the heat source base area. Nevertheless, even with much smaller heat transfer area, notice that multiple impinging jets display thermal performances similar to circular pin-fins at relatively large pumping power values.

Fig. 9, which presents a comparison of the cooling technologies at a pressure drop of 90 kPa, shows similar trends, however with lower thermal resistances and higher pumping power consumptions.

Figs. 10 and 11 show comparisons of the cooling technologies with HFE-7000 as the coolant. As expected, HFE-7000 performs poorly compared to water with total thermal resistance values much higher than those with water for a given pumping power. Similar to water, the offset strip fins outperform the other cooling technologies. Pin-fin arrangement has little to no effect on the thermal performance of the circular pin-fins. The micro-channels, compared to impinging jets, have better thermal performance for a wider range of total thermal resistances. This further highlights the complex nature of the thermal design optimization and the selection of electronics cooling technologies for a given application as the choice of the coolant not only dictates the maximum heat flux that can be dissipated but, also affects the selection of the cooling technologies.

4. Conclusions

A comprehensive comparative analysis of various electronics cooling technologies has been presented. The conclusions drawn from this study are subject to the imposed optimization constraints and the generality of the heat transfer and friction factor models used. In all cases studied, there is a trade-off between the total thermal resistance and pumping power consumption. The nature of this trade-off, however, is different from one cooling system to another. The main conclusions drawn from this study are as follows:

- Heat transfer and friction factor models used in present study are found to be reasonably valid for the range of operational conditions studied. The validity of Manglik and Bergles' correlations [19] has not been yet extensively extended to liquids and micro-scale configurations. Thus more numerical and experimental studies with liquids at the micro-scale should be done to study the extent of their correlations.
- Single objective optimization of either the thermal resistance or pumping power may not necessarily yield optimum performance. The multiple-objective optimization approach is preferable as it provides a solution with different trade-offs among which designers can choose from to meet their cooling needs.

- The choice of a coolant has a significant effect on the selection of a cooling technology for a particular cooling application and should, therefore, be taken into consideration along with other design factors, such as geometric configuration, system mass, volume, cost, manufacturability, and environmental benevolence.
- In general, the offset strip fin heat sink outperformed the other cooling technologies. Next to the offset strip fin heat sink in performance are the staggered and in-line circular pin-fin heat sinks, with the staggered arrangement displaying slightly better performance than the in-line arrangement. For relatively very low pumping powers, the micro-channel heat sinks offer lowest thermal resistances.
- Jet impingement cooling yields very high heat transfer coefficients. However, to make efficient use of this technology, it should be coupled with sufficiently large heat transfer surface area to increase the product hA_h.

Acknowledgements

This work is supported by the Office of Naval Research (ONR) under the Multidisciplinary University Research Initiative (MURI) Award GG10919 entitled "System-Level Approach for Multi-Phase, Nanotechnology-Enhanced Cooling of High-Power Microelectronic Systems." Support from Rensselaer Polytechnic Institute is also appreciated.

References

[1] B. Agostini, M. Fabbri, J.E. Park, L. Wojtan, J.R. Thome, B. Michel, State of the art of high heat flux cooling technologies, Heat Transfer Eng. 28 (2007) 258–281.
[2] D.K. Kim, S.J. Kim, Closed-form correlation for thermal optimization of microchannels, Int. J. Heat Mass Transfer 50 (2007) 5318–5322.
[3] W.A. Khan, J.R. Culham, Optimization of pin-pin heat sinks using entropy generation minimization, IEEE Trans. Compon. Packag. Technol. 28 (2005) 247–254.
[4] D.Y. Lee, K. Vafai, Comparative analysis of jet impingement and microchannel cooling for high heat flux applications, Int. J. Heat Mass Transfer 42 (1999) 1555–1568.
[5] D.B. Tuckerman, R.F.W. Pease, High-performance heat sinking for VLSI, IEEE Electron. Device Lett. EDL-2 (1981) 126–129.
[6] R.J. Phillips, Microchannel heat sinks, in: A. Bar-Cohen, A.D. Kraus (Eds.), Advances in Thermal Modeling of Electronic Components and Systems, ASME Press, New York, 1990 (Chapter 3).
[7] G.L. Morini, Single-phase convective heat transfer in microchannels: a review of experimental results, Int. J. Thermal Sci. 43 (2004) 631–651.
[8] R.W. Knight, J.S. Goodling, D.J. Hall, Optimal thermal design of forced convection heat sinks – analytical, J Electro. Packag. 113 (1991) 313–321.
[9] R.W. Knight, D.J. Hall, J.S. Goodling, R.C. Jaeger, Heat sink optimization with application to microchannels, IEEE Trans. Compon Hybrids Manufact. Technol. 15 (1992) 832–842.
[10] S.J. Kim, Methods for thermal optimization of microchannel heat sinks, Heat Transfer Eng. 25 (2004) 37–49.
[11] S.J. Kim, J.M. Hyun, A porous medium approach for the thermal analysis of heat transfer devices, in: D.B. Ingham, I. Pop (Eds.), Transport Phenomena in Porous Media III, Elsevier, New York, 2005 (Chapter 5).
[12] A. Husain, K.Y. Kim, Multiobjective optimization of a microchannel heat sink using evolutionary algorithm, J. Heat Transfer 130 (2008) 114505 (3 pages).
[13] A. Weisberg, H.H. Bau, Analysis of microchannels for integrated cooling, Int J. Heat Mass Transfer 35 (1992) 2464–2474.
[14] J.H. Ryu, D.H. Choi, S.J. Kim, Three-dimensional numerical optimization of a manifold microchannel heat sink, Int J. Heat Mass Transfer 46 (2003) 1553–1562.
[15] K. Foli, T. Okabe, M. Olhofer, Y. Jin, B. Sendhoff, Optimization of micro heat exchanger: CFD, analytical approach and multi-objective evolutionary algorithms, Int. J. Heat Mass Transfer 49 (2006) 1090–1099.
[16] A. Zukauskas, Heat transfer from tubes in crossflow, in: J.P. Hartnett, T.F. Irvine (Eds.), Advances in Heat Transfer, vol. 8, Springer, Berlin, 1972, pp. 93–160.
[17] A. Zukauskas, R. Ulinskas, Heat Transfer in Tube Banks in Crossflow, Hemisphere, Washington, 1988.
[18] W.M. Kays, A.L. London, Compact Heat Exchangers, McGraw Hill, New York, 1964.
[19] R.M. Manglik, A.E. Bergles, Heat transfer and pressure drop correlations for the rectangular offset strip fin compact heat exchanger, Exp. Thermal Fluid Sci. 10 (1995) 171–180.
[20] D.E. Metzger, R.A. Barry, J.P. Bronson, Developing heat transfer in rectangular ducts with staggered arrays of short pin-fins, ASME Trans. J. Heat Transfer 104 (1982) 700–706.
[21] J. Dong, J. Chen, Z. Chen, Y. Zhou, Air-side thermal hydraulic performance of offset strip fin aluminum heat exchangers, Appl. Thermal Eng. 27 (2007) 306–313.
[22] S.Y. Won, G.I. Mahmood, P.M. Ligrani, Spatially-resolved heat transfer and flow structure in a rectangular channel with pin fins, Int. J. Heat Mass Transfer 47 (2004) 1731–1743.
[23] A. Kosar, C. Mishra, Y. Peles, Laminar flow across a bank of low aspect ratio micro pin fins, J. Fluids Eng. 127 (2005) 419–430.
[24] A. Bejan, A.M. Morega, Optimal arrays of pin fins and plate fins in laminar forced convection, ASME J. Heat Transfer 115 (1993) 75–81.
[25] B.A. Jubran, M.A. Hamdan, R.M. Abdullah, Enhanced heat transfer, missing pin, and optimization for cylindrical pin fin arrays, ASME J. Heat Transfer 115 (1993) 576–583.
[26] M.A. Tahat, Z.H. Kodah, B.A. Jarrah, S.D. Probert, Heat transfer from pin-fin arrays experiencing forced convection, Appl. Energy 67 (2000) 419–442.
[27] R.K. Jha, S. Chakraborty, Genetic algorithm-based optimal design of plate fins following minimum entropy generation considerations, in: Proceedings of the IMECHE Part C Journal of Mechanical Engineering Science, vol. 219, Institution of Mechanical Engineers (2005), pp. 757–765.
[28] C.F. Ma, Y.P. Gan, Y.C. Tian, D.H. Lei, T. Gomi, Liquid jet impingement heat transfer with or without boiling, J. Thermal Sci. 2 (1993) 32–49.
[29] Y.Y. San, M.D. Lai, Optimum jet-to-jet spacing of heat transfer for staggered arrays of impinging air jets, Int. J. Heat Mass Transfer 44 (2001) 3997–4007.
[30] M. Fabbri, V.K. Dhir, Optimized heat transfer for high power electronic cooling using arrays of microjets, J. Heat Transfer 127 (2005) 760–769.
[31] A.J. Robinson, E. Schnitzler, An experimental investigation of free and submerged miniature liquid jet array impingement heat transfer, Exp. Thermal Fluid Sci. 32 (2007) 1–13.
[32] H. Jonsson, B. Moshfegh, Modeling of the thermal and hydraulic performance of plate fin, strip fin, and pin fin heat sinks – influence of flow bypass, IEEE Trans. Compon. Packag. Technol. 24 (2001) 142–149.
[33] K.S. Yang, W.H. Chu, I.Y. Chen, C.C. Wang, A comparative study of the airside performance of heat sinks having pin fin configurations, Int. J. Heat Mass Transfer 50 (2007) 4661–4667.
[34] W.A. Khan, J.R. Culham, M.M. Yovanovich, The role of fin geometry in heat sink Performance, J. Electron. Packag. 128 (2006) 324–330.
[35] N. Sahiti, F. Durst, P. Geremia, Selection and optimization of pin cross-sections for electronics cooling, Appl. Thermal Eng. 27 (2007) 111–119.
[36] C.Y. Li, S.V. Garimella, Prandtl-number effects and generalized correlations for confined and submerged jet impingement, Int. J. Heat Mass Transfer 44 (2001) 3471–3480.
[37] W.A. Khan, Modeling of fluid flow and heat transfer for optimization of pin-fin heat sinks, PhD Thesis, University of Waterloo, Waterloo, Ontario, Canada, 2004.
[38] S.V.J. Narumanchi, V. Hassani, D. Bharathan, Modeling Single-Phase and Boiling Liquid Jet Impingement Cooling in Power Electronics, NREL/TP-540-38787, National Renewable Energy Laboratory, Golden, Colorado, Dec. 2005.
[39] Genetic Algorithm and Direct Search Toolbox for use with MATLAB, User's Guide, Version 1, Release 13SP1+, The Mathworks Inc., 2004.
[40] A. Husaina, K.Y. Kim, Optimization of a microchannel heat sink with temperature dependent fluid properties, Appl. Thermal Eng. 28 (2008) 1101–1107.
[41] Y. Peles, A. Kosar, C. Mishra, C.J. Kuo, B. Schneider, Forced convective heat transfer across a pin fin micro heat sink, Int. J. Heat Mass Transfer 48 (2005) 3615–3627.
[42] M. Wong, I. Owena, C.J. Sutcliffe, A. Puri, Convective heat transfer and pressure losses across novel heat sinks fabricated by Selective Laser Melting, Int. J. Heat Mass Transfer 52 (2009), 281–288.
[43] A.B. Cohen, R. Bahadura, M. Iyengar, Least-energy optimization of air-cooled heat sinks for sustainability-theory, geometry and material selection, Energy 31 (2006) 579–619.
[44] H.M. Joshi, R.L. Webb, Heat transfer and friction in the offset strip-fin heat exchanger, Int. J. Heat Mass Transfer 30 (1987) 69–84.
[45] A.M. Jacobi, R.K. Shah, Heat transfer surface enhancements through the use of longitudinal vortices: a review of recent progress, Exp. Thermal Fluid Sci. 11 (1995) 295–309.